Paper

Two-Dimensional Nanoscale Imaging of Sugar Distribution Using AFM Force Sensing with Probe Modified by *Concanavalin A*

Shigeto Inoue,[1, 2] Yoshio Nakahara,[1] Shinpei Kado,[1] Mutsuo Tanaka,[3] and Keiichi Kimura[1]*

[1]*Department of Applied Chemistry, Faculty of Systems Engineering, Wakayama University, 930 Sakae-dani, Wakayama 640-8510, Japan*

[2]*Analytical Science Research Laboratories, Kao Corporation, 1334 Minato, Wakayama 640-8580, Japan*

[3]*Advanced Industrial Science and Technology, Central 5, 1-1-1 Higashi, Tsukuba, Ibaraki 305-8565 Japan*

*kkimura@center.wakayama-u.ac.jp

We have recently realized the two-dimensional visualization of a oligoethyleneglycol (*OEG*)/mannose (*Man*)-terminated pattern surface by performing AFM force measurements using a *concanavalin A* (*ConA*)-modified AFM tip. To extend the visualization technique, various types of patterned surfaces with localized sugar chains were fabricated by lithography and their two-dimensional visualizations were challenged in a phosphate-buffered saline solution by AFM force measurements using a *ConA*-modified AFM tip in this study. The adhesion force based on the interaction of *ConA* with *Man* was much larger than that based on the interaction of *ConA* with phosphorylcholine or galactose. The spatial resolution of this method was evaluated using a nanopatterned surface fabricated using silica nanoparticles. *Man*-terminated regions were clearly distinguishable from *OEG*-terminated regions on a nanometer scale.

1. Introduction

The structure of sugar chains on glycoproteins and glycolipids is one of the determining factors for biological reactions on cell surfaces since intercellular communication is thought to occur when sugar-binding proteins (lectins) recognize sugar chains on a cell surface. Sugar chain recognition by lectin has also been found to play key roles in pathological processes including inflammatory and immunological responses, cell–cell recognition, cancer metastasis, and viral infection [1–3]. Recent advances in mass spectrometric techniques have allowed compositional and structural changes of sugar chains that induce various responses to be elucidated, resulting in a deeper understanding of signal transduction and functional expression [4–5]. However, little is known about the two-dimensional distributions of sugar chains on biological surfaces in an aqueous environment on micrometer to nanometer scales due to their complexity and diversity.

Advanced analytical methods have been used to observe the dynamics and distributions of sugar chains on cell membranes. Lens-based fluorescence microscopy would be an ideal method for investigations on a subcellular level below 250 nm [6,7], except that since fluorescence techniques require fluorescent labeling of sugar chains, they are not direct analytical methods. Electron microscopy can be used to observe fine structures of sugar chains in cell membranes, but observations must be performed in a high vacuum. As gold nanoparticles interact specifically with sugar chains, an analytical method for investigating sugar chains has been developed that involves evaluating the distribution of gold nanoparticles adsorbed on cell membranes by scanning electron microscopy [8]. However, this method requires special equipment to be performed in the atmosphere. Thus, it is currently very difficult to observe the two-dimensional distributions of sugar chains on biological membranes in an aqueous environment.

Atomic force microscopy (AFM), which can be easily performed in an aqueous environment, is a

Journal of Surface Analysis Vol. 18 No. 3 (2012) pp. 164-173

S. Inoue et al.   Two-Dimensional Nanoscale Imaging of Sugar Distribution Using AFM Force Sensing with…

promising method for obtaining *in-situ* high-resolution images of surface structures [9]. In addition, AFM force spectroscopy is widely used in various fields to detect interaction forces between two compounds. For example, AFM force studies on specific host–guest interactions in artificial host molecules (e.g., cyclodextrin [10], crown ether [11], and calixarene [12]) have been performed. In recent years, recognition phenomena in biomolecules including ligand–receptor binding [13], antigen–antibody interaction [14], sugar chain–lectin recognition [15], protein unfolding [16], cell–protein interaction [17] and cell adhesion [18] have been investigated by AFM force measurements. In these measurements, a biomolecule is attached to an AFM tip and it is used to probe a surface modified by a comprehensive biomolecule.

Lectins are proteins that can recognize specific sugar chains and are thus very useful probes for studying sugar chains on cell surfaces [1]. In particular, *concanavalin A* (*ConA*) is a well-known lectin with specific affinities for α-D-mannosyl and α-D-glucosyl residues [19]. The interaction forces between *ConA* and corresponding simple sugars have been studied by AFM [15,20]. Furthermore, the two-dimensional visualization of the sugar chain distribution has been attempted using the force–volume technique [21]. However, it has not been adequately verified whether the force–volume images obtained in these studies accurately depict the sugar chain distribution. To confirm the validity of these images, it is necessary to use a sugar-patterned surface whose structure has been unambiguously determined. Against this background, we have recently realized the two-dimensional visualization of a mannose (*Man*)/oligoethyleneglycol (*OEG*)-terminated pattern surface by performing AFM force measurements using a *ConA*-modified AFM tip [22]. As the structure of the patterned surface was clearly known here, we confidently concluded that the mapping based on the specific interaction force between *ConA* and *Man* accurately depict the sugar
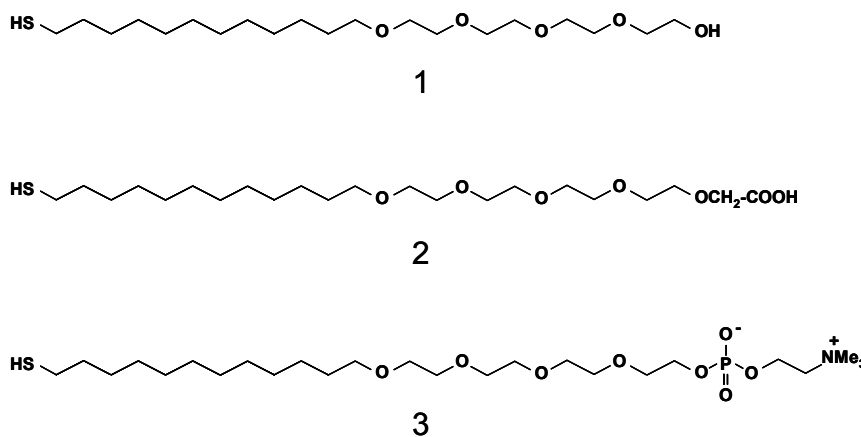

Figure 1. Molecular structure of functionalized thiol derivatives used in this study.

chain distribution. The present study seeks to extend our visualization technique. Various types of sugar-patterned surfaces were fabricated using functionalized thiol derivatives (Figure 1) and their two-dimensional distributions were visually mapped in a phosphate-buffered saline (PBS) on micrometer and nanometer scales by performing AFM force measurements using a *ConA*-modified AFM tip.

2. Experimental
2.1 Materials

Highly purified *concanavalin A*, D-(+)-mannose, ammonium carbonate, *N*-hydroxysuccinimide (NHS), and water-soluble carbodiimide hydrochloride (WSC) were purchased from Sigma-Aldrich (St. Louis, MO, USA). Amination of mannose was performed by the Kochetkov reaction [23]. PBS (pH 7.4) was purchased from Takara Bio (Tokyo, Japan). Deionized water (conductivity: 18 MΩ cm^{-1}) was prepared using a Milli-Q system. D-Mannosamine hydrochloride and D-galactosamine hydrochloride were purchased from Nacalai Tesque (Kyoto, Japan). Tetraethylene glycol/dodecane conjugate thiol **1**, acetic acid/tetraethylene glycol/dodecane conjugate thiol **2**, and phosphorylcholine (*PPC*)/tetraethylene glycol/dodecane conjugate thiol **3** (Figure 1) were prepared by the method given in Ref. 24. As sugar chains seem to be surrounded by *PPC* group of phospholipids moieties on the real biological membrane, mixed SAMs were also used in this study. Mica pieces were purchased from Merck (Darmstadt,

Journal of Surface Analysis Vol. 18 No. 3 (2012) pp. 164-173

S. Inoue et al.   Two-Dimensional Nanoscale Imaging of Sugar Distribution Using AFM Force Sensing with…

Germany). They were typically 5–15 µm in width and length. Silica nanoparticles (diameters: 50 and 100 nm) were kindly donated by Fuso Chemical Co., Ltd. (Osaka, Japan). Silicon substrates were purchased from Nilaco Co. (Tokyo, Japan).
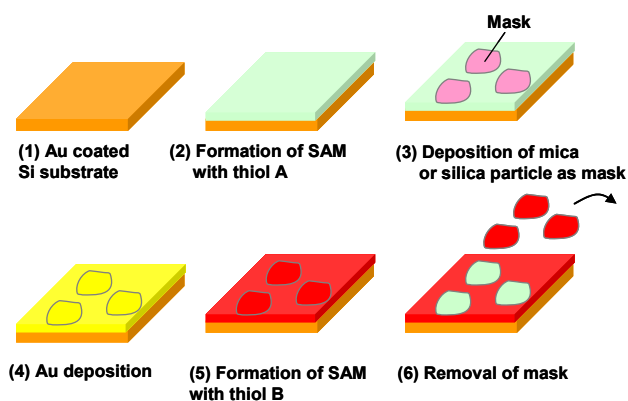

Figure 2. Schematic drawing of fabrication procedure of patterned substrate.

2.2 Preparation of PPC/Man-terminated patterned surface

The sugar-patterned surfaces were fabricated on a gold-coated silicon substrate by the lithography method shown as follows. Figure 2 shows a schematic diagram of the method. A gold-coated (50 nm) silicon substrate was immersed in an ethanol solution containing compound **3** (1.0 mM) for 24 h. The resulting self-assembled monolayer (SAM) was rinsed with ethanol and dried with nitrogen. Next, mica pieces were deposited on the substrate. A gold layer was then deposited on the substrate by vacuum evaporation and the substrate was immersed in an ethanol solution containing compounds **2** (1.0 mM) and **3** (1.0 mM) for 24 h. The substrate was immersed for 30 min in an aqueous solution of WSC (0.10 M) and NHS (0.10 M). Following activation of the terminal COOH, the substrate was rinsed with deionized water, dried with nitrogen, and immersed in an aqueous solution containing mannosylamine (1.0 mM) for 3 h. After rinsing with deionized water and drying with nitrogen, the mica pieces were removed from the substrate under running water.

2.3 Preparation of Man/Gal-terminated patterned surface

Man/*Gal*-terminated patterned surface was prepared by a similar method to that used to prepare the *PPC*/*Man*-terminated patterned surface. A gold-coated silicon substrate was immersed in an ethanol solution containing compounds **1** (1.0 mM) and **2** (1.0 mM) for 24 h. After chemical modification by mannosamine, mica pieces were deposited on the substrate. A gold layer was then deposited on the substrate by vacuum evaporation and immersed in an ethanol solution containing compounds **1** (1.0 mM) and **2** (1.0 mM) for 24 h. After chemical modification by galactosamine, mica pieces were removed from the substrate under running water.

2.4 Preparation of OEG/Man-terminated nanopatterned surface

An *OEG*/*Man*-terminated pattern surface was prepared by a similar method to that used to prepare the *PPC*/*Man*-terminated pattern surface with a minor modification. A gold-coated silicon was immersed in an ethanol solution containing compound **1** (1.0 mM) for 24 h. After SAM formation, silica nanoparticles were deposited on the substrate. A gold layer was then deposited on the substrate by vacuum evaporation and immersed in an ethanol solution containing compounds **1** (1.0 mM) and **2** (1.0 mM) for 24 h. After chemical modification by mannosylamine for 3 h, the silica nanoparticles were removed from the substrate under running water.

2.5 AFM force measurements

Gold-coated AFM cantilevers with a nominal spring constant of 0.025 N/m (Olympus, Tokyo, Japan) were used for force measurements. Their spring constants were calibrated to be in the range 0.022–0.028 N/m using the thermal noise method. All force measurements were performed in a PBS solution (pH 7.4) using a NanoScope V Multimode AFM (Veeco, Santa Barbara, CA). All force curves were acquired using the AFM software provided by the manufacturer at a scan rate of 1 Hz. The surface delay (defined as the delay between when the loading force reaches the target value and when the probe starts to retract) was set to 1 s. A contact force of 200 pN and a ramp size of 200 nm were used. Force curves were collected by the force–volume technique described in

Journal of Surface Analysis Vol. 18 No. 3 (2012) pp. 164-173

S. Inoue et al.   Two-Dimensional Nanoscale Imaging of Sugar Distribution Using AFM Force Sensing with…

Ref. 25. This method allows force curves to be acquired as a function of the lateral position on the sample surface. A complete force curve was recorded at each position by raster scanning the AFM tip across the surface of the sample in a 64×64 point array. Height images (64×64 pixels) were simultaneously recorded by force–volume mapping. Following acquisition, AFM force–volume data were analyzed offline by a purpose-written program developed in our laboratory using Microsoft Visual Basic.

2.6 Chemical modification of AFM tip

A gold-coated AFM tip was immersed in an ethanol solution containing compound **2** (1.0 mM) for 24 h and then rinsed with ethanol and dried with nitrogen. The tip was then immersed for 30 min in an aqueous solution containing WSC (0.10 M) and NHS (0.10 M). It was subsequently rinsed with deionized water and dried with nitrogen. Finally, the NHS-activated AFM tip was immersed in a PBS solution (pH 7.4) containing *ConA* (0.10 mg mL^{-1}) for 2 h and rinsed with a PBS solution.

3. Results and discussion
3.1 Fabrication of sugar-patterned surface

The alkanethiols spontaneously form self-assembled monolayers (SAMs) on a gold substrate. As sugar moieties can be easily introduced into functionalized SAMs with reactive sites using chemical reactions, several patterned SAMs containing sugar chains have been successfully constructed on gold substrates [26]. In our previous study, an *OEG*/*Man*-patterned surface was fabricated using compound **1** having an *OEG* end and compound **2** having a carboxylic group end through the condensation reaction with mannosylamine. However, real biological membranes do not have *OEG* chains; rather they have mixed surfaces with various phospholipids and other lipids. Therefore, a *PPC*/*Man*-patterned surface was prepared in this study using compound **3** with a *PPC* end with the aim of fabricating biomimetic surfaces. It is well known that *PPC* also suppresses the non-specific adsorption of proteins [27].

The sugar-patterned surfaces were fabricated on a gold-coated (50 nm) silicon substrate by lithography

using mica pieces or silica nanoparticles as masks [28]. Figure 2 shows a schematic diagram of the method used to fabricate the sugar-patterned surfaces. A gold-coated silicon substrate (1) was immersed in an ethanol solution containing thiol A for 24 h (2). The resulting SAM was rinsed with ethanol and dried with nitrogen. Next, mica or silica masks were deposited on the substrate (3). A gold layer was then deposited on the substrate by vacuum evaporation (4) and immersed in an ethanol solution containing thiol B for 24 h (5). Finally, the masks were removed from the substrate under running water (6). The completion of the pattern surface was confirmed by AFM topography. The terminal COOH of compound **2** was activated by immersion in an aqueous solution containing WSC and NHS for 30 min. After rinsing with deionized water and drying with nitrogen, aminated sugars were introduced to the substrate through a condensation reaction for 3 h.

3.2   Two-dimensional   mapping   of *PPC*/*Man*-terminated patterned surface

Figure 3 shows typical force curves obtained by *ConA*-modified tip for the *PPC*/*Man*-terminated pattern surface in a PBS solution. A characteristic adhesion force was obtained in the *Man*-terminated region that can be attributed to the specific adhesion force between *ConA* and *Man*; no such adhesion force was observed in the *PPC*-terminated region.
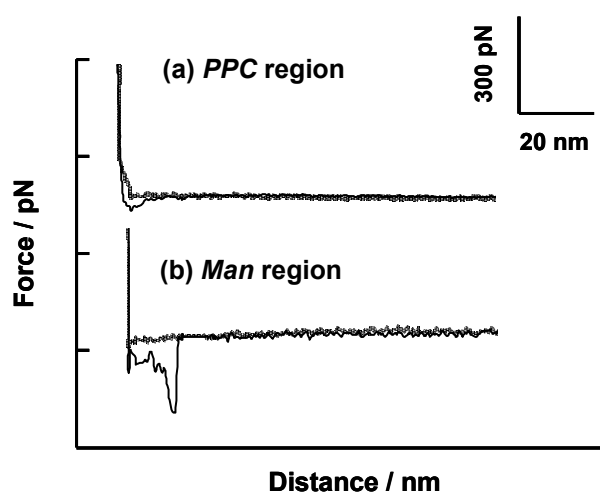

Figure 3. Typical AFM force curves obtained from (a) *PPC*-terminated, and (b) *Man*-terminated regions in a PBS solution.
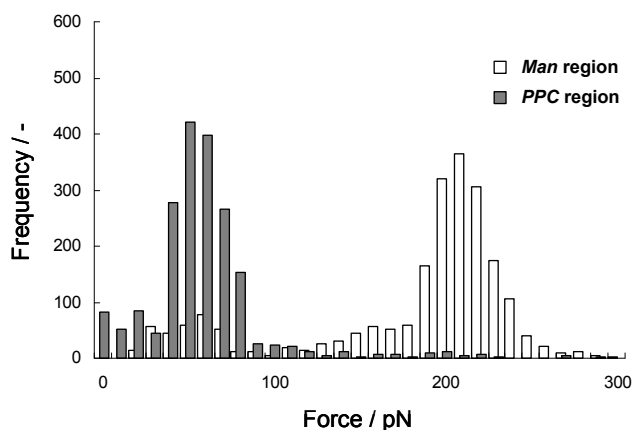
Figure 4. Histogram of adhesion forces obtained from *PPC*- and *Man*-terminated regions.
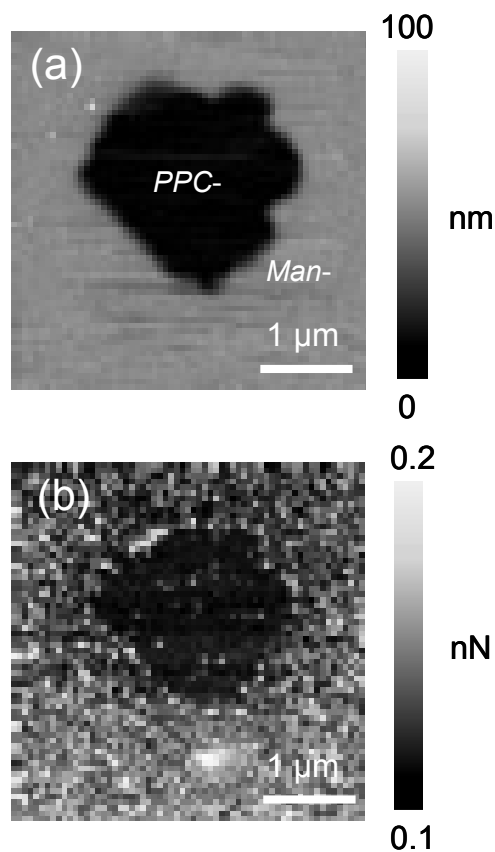

Figure 5. (a) Topological image and (b) adhesion force image of a *PPC/Man*-terminated patterned surface obtained using a *ConA*-modified tip in a PBS solution.

In the *Man*-terminated region, the specific adhesion force was approximately 200 pN (207 ± 27 pN), as shown in Figure 4. In contrast, in the *PPC*-terminated

region, the non-specific adhesion force was approximately 50 pN (55 ± 11 pN). The non-specific interaction forces observed in the *PPC*-terminated region were as large as those previously observed in the *OEG*-terminated region [19].

We were anxious about the interference from the hydrophobic interactions and electrostatic attractive forces between the *PPC* group and the hydrophobic protein, *ConA*. However, the present measurement revealed that this interaction force is considerably smaller than that between *ConA* and *Man*. Consequently, *Man*-terminated regions could be clearly distinguished from other regions, as shown in Figure 5. It was thus demonstrated that the *Man* distribution can be visualized even on a surface that is similar to a biological membrane.

3.3 Selective two-dimensional mapping of Man/Gal-terminated patterned surface

It is well known that *ConA* has a specific affinity for *Man* among other sugar residues. A *ConA*-modified tip has the potential to be used as a probe for selective AFM mapping of *Man* based on its specific affinity.

We prepared a mixed sugar-patterned surface of *Man* and *Gal* to investigate the ability of the *ConA*-modified tip to selectively visualize *Man* by this method. Figure 6 shows typical force curves for the *Man/Gal*-terminated pattern surface in a PBS solution.
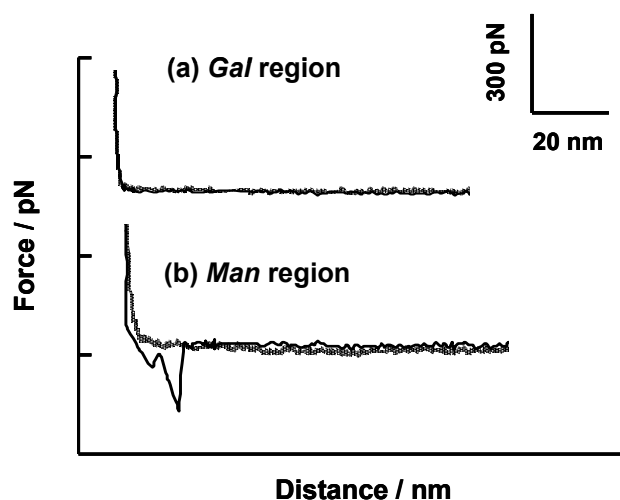

Figure 6. Typical AFM force curves obtained from (a) *Gal*-terminated, and (b) *Man*-terminated regions in a PBS solution.

Journal of Surface Analysis Vol. 18 No. 3 (2012) pp. 164-173

S. Inoue et al.   Two-Dimensional Nanoscale Imaging of Sugar Distribution Using AFM Force Sensing with…

No significant specific force was observed in the *Gal*-terminated region like the *PPC*-terminated region. Thus, the *Man*-terminated regions can be selectively visualized in the mixed sugar-patterned surface (Figure 7). Accordingly, it may be possible to detect other sugar chains by attaching different lectins to the AFM tip. For some lectins, the interaction force of lectin with biological membranes may be too strong to detect the specific interaction force with the sugar chain. Thus, for practical applications, it is necessary to confirm the detection ability of individual lectins by performing systematic investigations using the method presented here.
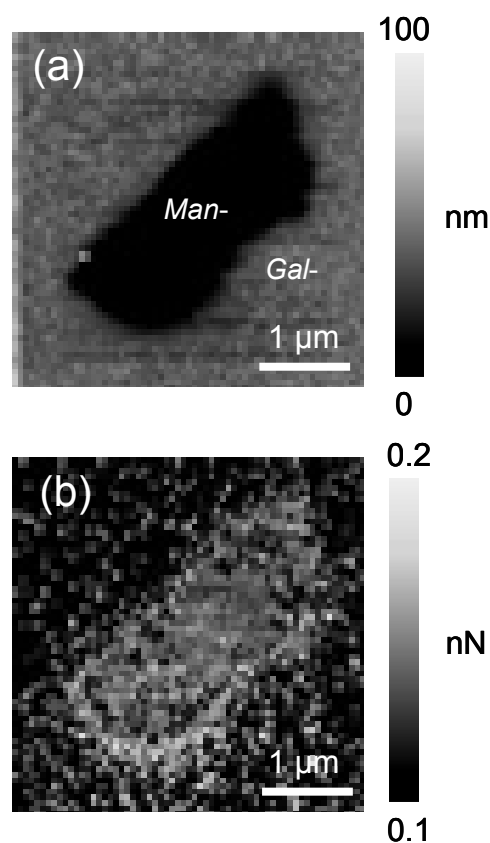

Figure 7. (a) Topological image and (b) adhesion force image of the *Man*/*Gal*-terminated patterned surface obtained with a *ConA*-modified tip in a PBS solution.

3.4 Evaluation of spatial resolution

The spatial resolution was evaluated using a sugar-patterned surface fabricated by colloidal lithography using silica nanoparticles with two different diameters (50 and 100 nm) as a mask. Figure 8 shows topological images and adhesion force images of

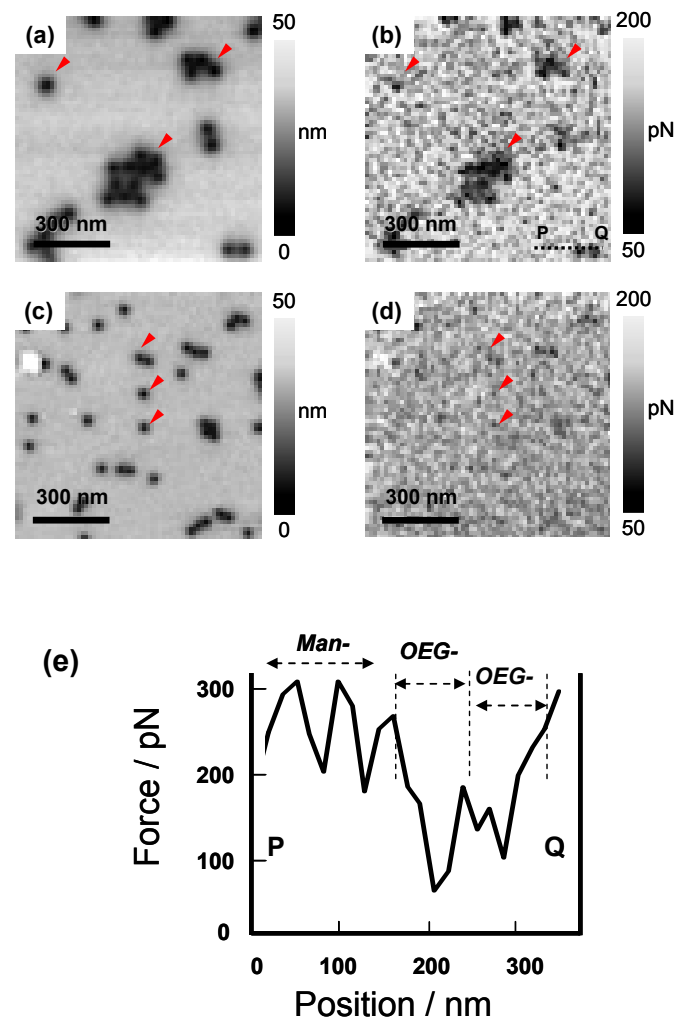the *OEG*/*Man*-terminated nanopatterned surfaces in a PBS solution.

Figure 8. (a) Height and (b) adhesion force images of *OEG*/*Man*-terminated nanopattern surface fabricated using 100-nm-diameter silica nanoparticles. (c) Height and (d) adhesion force images of the *OEG*/*Man*-terminated nanopattern surface fabricated using 50-nm-diameter silica nanoparticles. Arrows in the image indicate nanopatterned regions fabricated by silica nanoparticles. (e) Force line-profile of dotted P-Q line in (b). *Man* and *OEG* region are clearly distinguished.

In the topological images, the relatively high region is the *Man*-terminated region and the low region is the *OEG*-terminated region. Using the nanopatterned surface fabricated using 100-nm-diameter silica nanoparticles, it was confirmed that *Man*-terminated regions could be clearly identified by adhesion force

Journal of Surface Analysis Vol. 18 No. 3 (2012) pp. 164-173

S. Inoue et al.   Two-Dimensional Nanoscale Imaging of Sugar Distribution Using AFM Force Sensing with…

mapping (Figure 8b). In contrast, *Man*-terminated regions could not be clearly visualized for the nanopatterned surface fabricated using 50-nm-diameter silica nanoparticles (Figure 8d). This is presumably due to the non-negligible interactions with *Man* in the hole sidewalls, even when measuring a *OEG*-terminated region in the hole, because the tip diameter (10–20 nm) is very similar to the hole size. Furthermore, due to the size of *ConA* attached to the tip via an *OEG* chain, it would appear to be difficult to accurately detect regions that are several tens of nanometers in size using a *ConA*-modified AFM tip. Therefore, this method was determined to have an effective spatial resolution of approximately 100 nm.

4. Conclusion

Precisely sugar-patterned surfaces were fabricated by lithography and their two-dimensional distributions were successfully visualized in a PBS solution by AFM force measurements with a *ConA*-modified tip. *Man*-terminated regions could be distinguished from *PPC*-terminated regions on a surface that resembles a biological membrane. In addition, *Man*-terminated regions could also be distinguished from *Gal*-terminated regions, which demonstrates that target sugar chains can be selectively detected using an AFM tip chemically modified by the corresponding lectin. The spatial resolution of this technique was estimated to be approximately 100 nm using an *OEG*/*Man*-terminated nanopatterned surface fabricated using silica nanoparticles. We believe that the method proposed in this study will be used for distribution analysis of sugar chains in lipid rafts (size of lipid rafts: dozen nanometers to several micrometers in diameter) in the near future.

5. References

[1] A. Varki, *Glycobiology* **3**, 97 (1993).

[2] P. Gagneux, A. Varki, *Glycobiology* **9**, 747 (1999).

[3] B. K. Brandley, R. L. Schnaar, *J. Leukoc. Biol.* **40**, 97 (1986).

[4] A. Kameyama, N. Kikuchi, S. Nakaya, H. Ito, T. Sato, T. Shikanai, Y. Takahashi, K. Takahashi, H. Narimatsu, *Anal. Chem.* **77**, 4719 (2005).

[5] H. Ito, A. Kameyama, T. Sato, K. Kiyohara, Y. Nakahara, H. Narimatsu, *Angew. Chem. Int. Ed.* 44, 4547 (2005).

[6] S. W. Hell, J. Wichmann, *Opt. Lett.* **19**, 780 (1994).

[7] S. W. Hell, *Science* **316**, 1153 (2007).

[8] T. Murai, Y. Maruyama, K. Mio, H. Nishiyama, M. Suga, C. Sato, *J. Biol. Chem.* **286(3)**, 1999 (2011).

[9] G. Binnig, C. F. Quate, C. Gerber, *Phys. Rev. Lett.* **56**, 930 (1986).

[10] (a) H. Schönherr, M. W. J. Beulen, J. Bügler, J. Huskens, F. C. J. M. van Veggel, D. N. Reinhoudt, G. J. Vancso, *J. Am. Chem. Soc.* **122**, 4963 (2000). (b) S. Zapotoczny, T. Auletta, M. R. de Jong, H. Schönherr, J. Huskens, F. C. J. M. van Veggel, D. N. Reinhoudt, G. J. Vancso, *Langmuir* **18**, 6988 (2002). (c) T. Auletta, M. R. de Jong, A. Mulder, F. C. J. M. van Veggel, J. Huskens, Reinhoudt, D. N.; Zou, S.; Zapotoczny, S.; H. Schönherr, G. J.Vancso, L. Kuipers, *J. Am. Chem. Soc.* **126**, 1577 (2004).

[11] (a) S. Kado, K. Kimura, *J. Am. Chem. Soc.* **125**, 4560 (2003). (b) S. Kado, K. Yamada, K. Kimura, *Langmuir* **20**, 3259 (2004).

[12] R. Eckel, R. Ros, B. Decker, J. Mattay, D. Anselmetti, *Angew. Chem., Int. Ed.* **44**, 484 (2005).

[13] (a) S. Allen, J. Davis, A. C. Dawkes, M. C. Davis, J. C. Edwards, M. C. Parker, C. J. Roberts, J. Sefton, S. J. B. Tendler, P. M. Williams, *FEBS Lett.* **390**, 161 (1996). (b) S. S. Wong, E. Joselevich, A. T. Woolley, C. L. Cheung, C. M. Lieber, *Nature* **394**, 52 (1998). (c) C. Yuan, A. Chen, P. Kolb, V. T. Moy, *Biochem.* **39**, 10219 (2000).

[14] (a) U. Dammer, M. Hegner, D. Anselmetti, P. Sagner, M. Dreier, W. Huber, H. J. Guntherodt, *Biophys. J.* **70**, 2437 (1996). (b) Y. Harada, M. Kuroda, A. Ishida, *Langmuir* **16**, 708 (2000).

[15] A. Touhami, B. Hoffmann, A. Vasella, F. A. Denis, Y. F. Dufrêne, *Langmuir* **19**, 1745 (2003).

[16] (a) M. Rief, M. Gautel, F. Oesterhelt, J. M. Fernandez, H. E. Gaub, *Science* **276**, 1109 (1997). (b) T. M. Fisher, P. E. Marszalek, J. M. Fernandez, *Nat. Struct. Biol.* **7**, 719 (2000). (c) A. F. Oberhauser, M. Carrion-Vazquez, *J. Biol. Chem.* **283**, 6617 (2008).

[17] Y. Bustanji, C. R. Arciola, M. Conti, E. Mandello, L. Montanaro, B. Samori, *Proc. Natl. Acad. Sci. U.S.A.* **100**, 13292 (2003).

[18] E. A. Evans, D. Calderwood, *Science* **316**, 1148 (2007).

Journal of Surface Analysis Vol. 18 No. 3 (2012) pp. 164-173

S. Inoue et al.   Two-Dimensional Nanoscale Imaging of Sugar Distribution Using AFM Force Sensing with…

[19] H. Lis, N. Sharon, *Chem. Rev.* **98**, 637 (1998).

[20] (a) M. Lekka, P. Laidler, J. Dulinska, M. Labedz, G. Pyka, *Eur. Biophys. J. Biophys. Lett.* **33**, 644 (2004). (b) T. V. Ratto, K. C. Langry, R. E. Rudd, R. L. Balhorn, M. J. Allen, M. W. McElfresh, *Biophys. J.* **86**, 2430 (2004).

[21] (a) V. Dupres, F. D. Menozzi, C. Locht, B. H. Clare, N. L. Abbott, S. Cuenot, C. Bompard, D. Raze, Y. F. Dufrêne, *Nat Methods* **2**, 515 (2005). (b) Y. Gilbert, M. Deghorain, L. Wang, B. Xu, P. D. Pollheimer, H. J. Gruber, J. Errington, B. Hallet, X. Haulot, C. Verbelen, P. Hols, Y. F. Dufrêne, *Nano Lett.* **7**, 796 (2007).

[22] S. Inoue, Y. Nakahara, S. Kado, M. Tanaka, K. Kimura, *J. Surf. Anal.* **17**, 328 (2011).

[23] L. Likhosherstov, O. Novikova, V. A. Derveitskaja, N. K. Kochetkov, *Carbohydr. Res.* **146**, c1 (1986).

[24] M. Tanaka, T. Sawaguchi, Y. Sato, K. Yoshioka, O. Niwa, *Tetrahedron Lett.* **50**, 4092 (2009).

[25] M. Radmacher, J. P. Cleveland, M. Fritz, H. G. Hansma, P. K. Hansma, *Biophys. J.* **66**, 2159 (1994).

[26] (a) X. Zhang, V. K. Yadavalli, *Anal. Chim. Acta.* **649**,1 (2009). (b) T. P. Sullivan, W. T. S. Huck, Eur. J. Org. Chem. 17 (2003). (c) S. Flink, F. C. J. M. van Veggel, D. N. Reinhoudt,Adv. Mater. 12, 1315 (2000).

[27] (a) K. Ishihara, T. Ueda, N. Nakabayashi, *Polymer J.* **22**, 355 (1990). (b) K. Ishihara, H. Nomura, T. Mihara, K. Kurita, Y. Iwasaki, N. Nakabayashi, *J. Biomed. Mater. Res.* **39**, 323 (1998).

[28] (a) M. Akiyama, M. Fujita, M. Fujihira, *Chem. Lett.* **35**, 1112 (2006). (b) S. Kado, H. Yano, Y. Nakahara, K. Kimura, *Chem. Lett.* **38**, 58 (2009).

査読コメント

査読者 1. 青柳里果（島根大学）

The manuscript describes chemically modified AFM for detecting a particular sugar chains. I have same comments:

［査読者 1-1］

Although it is indicated that the specific affinity of the modified AFM is effective for detecting the particular sugar, mannose, it is not mentioned if the method is feasible to detect real biological membranes or not. Please explain sizes of the target sugar chains in the biological membranes.

［著者］

Thank you for your comments. Target sugar chains on biological membranes are "lipid rafts" domain. Lipid rafts are several dozen nanometers to several micrometers. In this study, we showed that the spatial resolution of our technique was approximately 100 nm. So, we think that the method proposed in this study will be used for distribution analysis of sugar chains in lipid rafts in the near future.

［査読者 1-2］

Since proteins are supposed to be much larger than sugar chains, it would be difficult to detect a particular sugar on the membranes. Please mention your strategies to achieve enough spatial resolution using protein-modified tips.

［著者］

Thank you for your comment. As you know, in an AFM imaging, spatial resolutions are dependent on the probe size. So, it is very difficult to detect a single sugar chain at this stage. However, that point is one of the important technological opportunities, the development of another detection technique using a low molecular weight of host compound is underway.

［査読者 1-3］

Are there any solutions to detect unknown sugar on the membrane?

［著者］

It is very difficult to detect an unknown sugar chain at this stage, because our method is based on the detection of the specific interaction force between sugar recognition protein and "particular" sugar chain. This technical issue remains as one of the important key problems to be solved.

Journal of Surface Analysis Vol. 18 No. 3 (2012) pp. 164-173

S. Inoue et al.   Two-Dimensional Nanoscale Imaging of Sugar Distribution Using AFM Force Sensing with…

査読者 2. 藤平正道（東京薬科大学薬学部 客員教授，東京工業大学 名誉教授）

生体試料表面を模した，人工的な表面を作製し，糖鎖の化学識別を AFM で明確に観察した点は大いに評価されて良いと判断します．但し，以下の点を改訂されたらさらに良い論文になると思われます．

［査読者 2-1］

二つの異なった化学組成を持ち，かつ，一方の領域が 10 μm～100 nm スケールの部分表面からなる試料の調製法の説明が理解しにくい．理解を困難にする理由の一つに，Figure 2 の調製の説明図が Results and discussion の 3.1 で初めて出てくることにあります．この図の後に，2.2, 2.3 及び 2.4 の Experimental の記述がくれば，この調製法に不慣れな読者も容易に理解できると思われます．

［著者］

2.2 項の文頭に Figure 2 の説明図を示すように追記修正しました．また，Figure 2 の位置を 2.2 項の前にレイアウト変更しました．

［査読者 2-2］

何故，溶液中のチオール類による自己組織化膜（SAM）形成法を用いて本研究の目的を達成しようとしたかの動機が明確に記述されていません．出来れば簡単な説明を加えた方が良いと思われます．充分な時間がなければ，次回にはこの方法を用いる意義を明確にされることをお勧めします．

［著者］

3.1 項の文頭に，自己組織化膜（SAM）を用いた簡単な説明を追記しました．

［査読者 2-3］

金表面の化合物 1～3 による SAM 形成はかなり確立した表面化学修飾法であるので，本文（2.2～2.4）中の記述で充分であると思われますが，*Man* の導入に関する記述は少なくとも反応時間の記述が必要と思われます．このままでは他の研究者の追試は困難です．もしこの研究が継続されるのであれば，いずれは（次の論文では）*Man*, *Gal*, および *ConA* が化合物 2 の SAM 表面へ導入された事を示す，他の手法による表面分析結果の提示が望まれます．今回の力測定の結果が導入を示していると言うのでは，本法による糖鎖識別法の提案の意義を弱めます．何故，このようなコメントを

するかというと，その背景には「高密度に充填された化合物 3 に囲まれ，埋もれた化合物 2 の -COOH 末端はさらなる表面修飾反応に関与できるのか？」という疑問からです．*Man*, *Gal*, および *ConA* の面密度の知見もより定量的な議論には必要になると思われます．

［著者］

実験項に反応時間の記述を追記しました．

また，ご指摘の通り，*Man*, *Gal*, および *ConA* が SAM 表面へ導入されたことに関する実験的証拠を得ることが必要です．現在も表面分析法を用いた検討をいくつか行っていますが，今のところ固定化されていることを示す直接的な実験的証拠は得られておりません．

ConA の固定化については，現在のところ以下のように重ねて検証しています．

(i)　金基板に *ConA* を修飾した後に，飛行時間型二次イオン質量分析計（TOF-SIMS）を用いて基板表面から得られるマススペクトルを解析した結果，*ConA*（タンパク質）由来のフラグメントイオン CN⁻（*m/z* 26）が高強度で得られることを確認しました．よって，*ConA* が金基板に固定化されていることが示唆されます．

(ii)　*ConA* 修飾探針を用いて基板に固定化されたマンノースのセンシングを行い，特徴的なフォースカーブが得られている測定系中に，フリーのマンノースを導入すると，特徴的なフォースカーブが得られなくなることを確認しました（ブロッキング試験）．このことは，探針に修飾した *ConA* にフリーのマンノースが結合して，基板表面のマンノースと結合できなくなっていることを示唆しています．すなわち，探針には *ConA* が修飾されているものと判断されます．

(iii)　*ConA* を探針に修飾していない場合，Man と *ConA* 間に働く特徴的な相互作用力が得られないことを確認しています．すなわち，本報告で示した *ConA－Man* の相互作用力は，*Con A* が固定化された探針と *Man* との相互作用力であると判断されます．

Man や *Gal* についても同様に，固定化前後で得られるフォースカーブを比較した結果，固定化後にのみ特徴的な相互作用力が得られました．また，TOF-SIMS 測定を行い，糖鎖分子の直接検出につ

Journal of Surface Analysis Vol. 18 No. 3 (2012) pp. 164-173

S. Inoue et al.   Two-Dimensional Nanoscale Imaging of Sugar Distribution Using AFM Force Sensing with…

いて検討しましたが，糖鎖分子イオンは検出されませんでした．糖鎖を検出するためには表面分析的な工夫（ソフトイオン化等）が必要と考えており，TOF-SIMS や表面分析の専門家の皆様と議論し，検討を進めたいと考えております．

[査読者 2-4]

Ref. 25 では上記の理由で，走査速度は 0.1 Hz を採用しています．今日の市販の装置では 1 Hz でも像を撮れるのですか？

[著者]

本論文で示している走査速度（1 Hz）は，フォースカーブ取得時の走査速度です．走査速度は，0.01～100 Hz 程度まで変化させることができ，これは過去から現在に至るまで大きく変化しておりません．Hansma らの走査速度 0.1 Hz という記述は，マッピング像を得る際の水平方向の走査速度ですので，ここで示したフォースカーブ測定の走査速度の意味合いとは異なっております．

[査読者 2-5]

The reverse delay は 1 s とありますが，もしフォースカーブに関連する時間であれば，1 ms ではありませんか？見当違いかもしれませんが，force-volume 法に関する記述に関しては，Ref.25 の出版時と今日の時間差を考慮しますと，もう少し丁寧に説明した方が読者には理解しやすいのではないでしょうか？

[著者]

本論文で記述しました"reverse delay"は，表面に探針が接触した後にそのまま待機させる時間を示しておりました（force-volume 法に付属する機能）．タンパク質の分子認識には時間依存性があり，今回用いている *ConA* と *Man* との相互作用

においては，1s 程度の時間接触させておくことが分子を認識する上で重要となります．このような背景に基づき，生体認識の相互作用力研究に force-volume 法が多用されております．従って，pulse-force-mode AFM は高速で相互作用力像が得られる大変有用な技術なのですが，本ターゲットにおいては不向きと判断しております．

なお，force-volume 法において，より一般的に用いられている"surface delay"という記述に改めました．

[査読者 2-6]

付着力は表面の凹凸によって分布を持つことが知られています（F. Sato et al., Ultramicroscopy 97, 303 (2003))．金の膜厚が厚くなると，金凸部の半径も増加し，益々付着力の分布が広がり，中心の力の平均値も変化します．この結果は「AFM 探針先端の球面と試料表面の凸部の上では球－球一点接触で，表面の球に囲まれた凹部では探針先端球が複数の表面球と多点接触することにより力の分布が観測される」と説明されます．この観点からは 50 nm は少々厚めかもしれません．付着力の凹凸依存性は Hasma らの文献 25 でも指摘されています．今後は凹凸の影響も考慮して付着力測定をされることをお勧めします．

[著者]

ご指摘頂いた点は，今後付着力の定量的な議論を深めていく際に極めて重要であると思います．今後の検討では，凹凸の影響を出来るだけ低減できるような試料調製法を検討していきたいと考えております．その手段の一つとして，今回ご教示頂いた金の膜厚制御を行い，系統的に評価を行っていきたいと考えております．